Polycaprolactone-Coated 3D Printed Tricalcium Phosphate Scaffolds for Bone Tissue Engineering: *In Vitro* Alendronate Release Behavior and Local Delivery Effect on *In Vivo* Osteogenesis

Solaiman Tarafder and Susmita Bose*

W. M. Keck Biomedical Materials Research Laboratory, School of Mechanical and Materials Engineering, Washington State University, Pullman, Washington 99164, United States

Ⓢ *Supporting Information*

ABSTRACT: The aim of this work was to evaluate the effect of *in vitro* alendronate (AD) release behavior through polycaprolactone (PCL) coating on in vivo bone formation using PCL-coated 3D printed interconnected porous trical-cium phosphate (TCP) scaffolds. Higher AD and Ca^{2+} ion release was observed at lower pH (5.0) than that at higher pH (7.4). AD and Ca^{2+} release, surface morphology, and phase analysis after release indicated a matrix degradation dominated AD release caused by TCP dissolution. PCL coating showed its effectiveness for controlled and sustained AD release. Six different scaffold compositions, namely, (i) TCP (bare TCP), (ii) TCP + AD (AD-coated TCP), (iii) TCP + PCL (PCL-coated TCP), (iv) TCP + PCL + AD, (v) TCP + AD + PCL,

and (vi) TCP + AD + PCL + AD were tested in the distal femoral defect of Sprague−Dawley rats for 6 and 10 weeks. An excellent bone formation inside the micro and macro pores of the scaffolds was observed from histomorphology. Histomorphometric analysis revealed maximum new bone formation in TCP + AD + PCL scaffolds after 6 weeks. No adverse effect of PCL on bioactivity of TCP and *in vivo* bone formation was observed. All scaffolds with AD showed higher bone formation and reduced TRAP (tartrate resistant acid phosphatase) positive cells activity compared to bare TCP and TCP coated with only PCL. Bare TCP scaffolds showed the highest TRAP positive cells activity followed by TCP + PCL scaffolds, whereas TCP + AD scaffolds showed the lowest TRAP activity. A higher TRAP positive cells activity was observed in TCP + AD + PCL compared to TCP + AD scaffolds after 6 weeks. Our results show that *in vivo* local AD delivery from PCL-coated 3DP TCP scaffolds could further induce increased early bone formation.

KEYWORDS: *tricalcium phosphate (TCP), 3D printing (3DP), in vitro alendronate release, polycaprolactone (PCL) coating, in vivo osteogenesis*
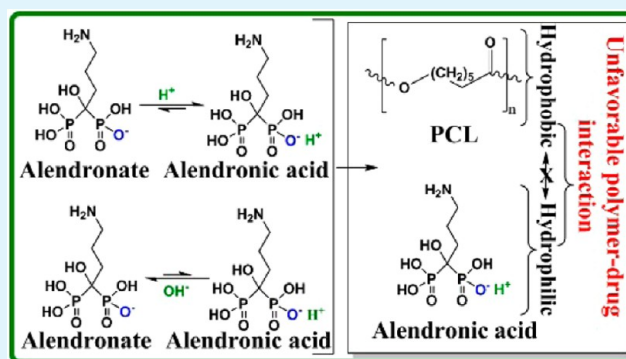
1. INTRODUCTION

Ever increasing rate of musculoskeletal diseases and disorders caused by bone tumors, trauma, disease, birth defects and war, or traffic injuries often times require treatment with an appropriate drug for accelerated healing or preventing post-operative infections. The shortcomings of systemic drug delivery, such as low bioavailability and low efficacy can cause unwanted potential side effects.[1,2] Systemic delivery requires the periodic intake of high-dose drugs because of low bioavailability.[3] Reduced side effects, improved bioavailability, and efficacy can be achieved by local drug delivery.[4,5] Small osteogenic drug molecules or growth factors are of increased interest because of their potential use in hard tissue repair or regeneration applications.[6] The wide use of synthetic bi-sphosphonates (BPs) in the treatment of various skeletal disorders, such as osteoporosis, tumor-associated osteolysis, Paget's disease, and hypercalcemia, is because of their potent

inhibition of bone resorption.[1,7] The backbone of BPs are structurally similar to inorganic pyrophosphate.[8]

Alendronate (AD), a member of the bisphosphonate family, is one of the most commonly used drug for osteoporosis.[9] While most BPs including AD contain nitrogen in the structure, non-nitrogen containing BPs also exist. Although both nitrogen and non-nitrogen containing BPs act on preventing bone resorption by inhibiting osteoclast activity, their mechanism of action is different.[10] Nitrogen containing BPs are believed to inhibit farnesyl diphosphate synthase (FPP synthase) in the mevalonate to cholesterol synthesis pathway.[10,11] Downstream intermediate biomolecules that are essential for cholesterol synthesis in the mevalonate pathway can be blocked through inhibition of FPP synthase.[12,13] It has been shown that
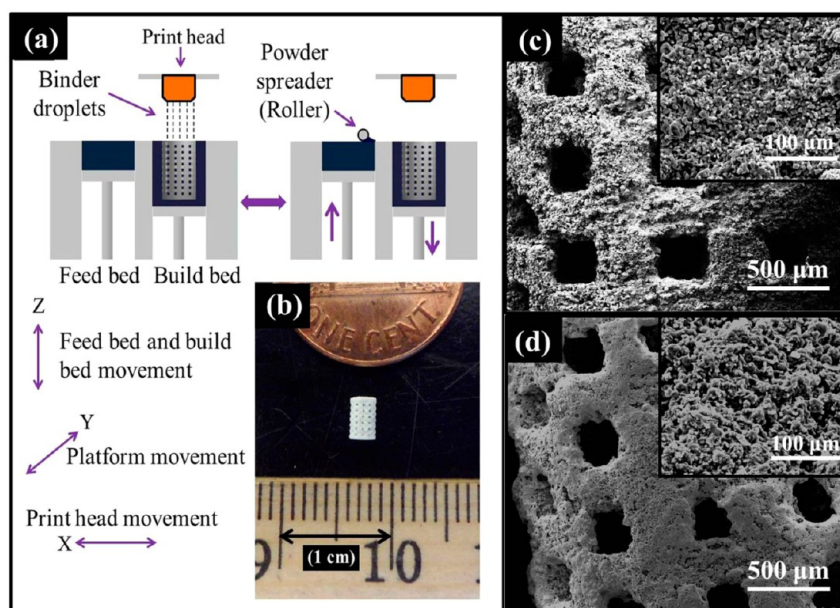
Figure 1. (a) Schematic of 3D printing (3DP), (b) sintered 3DP TCP scaffold, and (c, d) surface morphology of the 3D printed bare TCP and PCL-coated 3D printed TCP scaffolds, respectively.

geranylgeranyl pyrophosphate, a downstream intermediate of the mevalonate to cholesterol synthesis pathway, exerts a stimulatory effect on bone resorbing osteoclast cells activities.[6] Therefore, the osteoclasts activities suppression by AD is the result of inhibition of geranylgeranyl pyrophosphate synthesis required for osteoclasts stimulation.[14,15] Early stage osteo-genesis can thus be induced by local delivery of BPs as a result of osteoclast activity inhibition[16] along with reducing the bone fracture risk from osteoporosis.[1,17] New induced bone formation by BPs due to osteoclast activity inhibition can lead to quicker recovery after surgery as a result of improved mechanical interlocking between implant and the surrounding host tissue.

Excellent bioactivity of CaPs and compositional similarities to bone mineral are the reasons for their wide use and preferred choice for hard tissues, such as teeth or bone repair, replacement, regeneration, or augmentation.[18–21] The in-creased interest in CaPs to use as drug delivery systems (DDSs) in orthopedics, dentistry, and nanomedicine is because of their versatility and tailorable biodegradability over other ceramics.[1,2,22,23] Sustained and controlled release of drugs or osteogenic factors from scaffolds are required over a desired period of time for an effectual treatment. In burst release kinetics, most of the drug is released over a very short period of time leading to a detrimental or no effect to the target site or tissue. Burst release from CaP scaffolds can be inhibited by embracing a polymeric coating approach, where the polymer is biodegradable.[1,24–26] There are two potential approaches, the polymer coating itself can incorporate the drug molecules or the coating can be applied on a drug treated surface.[1] Tissue engineering scaffold materials should be biodegradable, non-immunogenic, non-carcinogenic, and non-toxic with excellent cell/tissue biocompatibility. Semi-crystalline polycaprolactone (PCL) meets these criteria. Moreover, it is a low cost and easy to process material. Thus, it is not a surprise that PCL is being widely explored for tissue engineering and drug delivery applications.[27,28] Our recent work on *in vitro* release behavior of lovastatin (an osteogenic drug) from polycaprolactone

(PCL) coated dense tricalcium phosphate (TCP) showed release was controlled by drug-polymer interactions, which was dependent on the drug polymer hydrophilic hydrophobic interactions. This influenced the drug release kinetics from PCL-coated TCP disc[6] showing *in vitro* controlled release kinetics of lovastatin. Architectural features of tissue engineer-ing scaffolds are critical components that need to be taken care of during fabrication.

The presence of three dimensionally interconnected macro pores facilitate new tissue ingrowth throughout the entire scaffold, which provides enhanced mechanical interlocking between surrounding host tissue and the scaffold. Pore interconnectivity allows nutrient and metabolic waste transport to and from the core of the scaffold, which is very crucial for proper vascularization. Fabrication of CaP scaffolds with complex and controlled geometrical features by conventional techniques is a challenging task since pore size, interconnec-tivity, distribution, and volume fraction porosity is difficult to control precisely.[29–32] In our earlier work,[29] we reported that CaP scaffolds with different designed macropore sizes can successfully be fabricated using 3D printing (3DP) technology, where we optimized 3D printing parameters, such as layer thickness, binder saturation, drop volume, roller spreading speed and drying time, to attain micro and macro porous scaffolds. Our results from that study[29] also showed that the mechanical strength of the 3DP designed macro porous TCP scaffolds can significantly be improved by microwave sintering as opposed to conventional sintering method.

Here, we examine the effect of PCL coating on *in vitro* alendronate (AD) release behavior, and local alendronate (AD) delivery on *in vivo* osteogenesis from PCL-coated 3D printed interconnected macro porous tricalcium phosphate (TCP) scaffolds. TCP scaffolds with interconnected designed macro pores were fabricated using 3D printing technique, and PCL was coated on AD adsorbed 3DP TCP scaffolds. Effect of PCL coating on the compressive strength and toughness of these 3DP TCP scaffolds was evaluated. *In vitro* AD release was investigated at physiological pH 7.4 and relatively acidic pH 5.0

from both bare (uncoated) and PCL-coated 3DP TCP scaffolds. Bioactivity of theses PCL-coated scaffolds was first investigated *in vitro* using human fetal osteoblast (hFOB) cells. To evaluate the effect of PCL coating on AD coated TCP, we have also compared this with uncoated TCP, TCP coated with only AD and only PCL. Finally, the effect of PCL and AD were examined on new bone formation and tartrate resistant acid phosphatase (TRAP) positive cells activity by histomorphology and histomorphometric analysis after 6 and 10 weeks post implantation in a rat distal femoral defect model.

2. MATERIALS AND METHODS

2.1. Scaffold Fabrication. β-TCP powder with 550 nm average particle size (Berkeley Advanced Biomaterials Inc., Berkeley, CA) were used for scaffold fabrication. Scaffolds with 350 μm designed pore size [scaffold dimension: 3.4 mm (ϕ) × 5.2 mm (h)] were fabricated. Square shaped designed interconnected macro pores were distributed orthogonally through the cylindrical shape in X, Y, and Z directions. A 3D printer (ExOne, Irwin, PA, USA) was used for scaffold fabrication. After 3D printing, the binder (organic based binder, purchased from ExOne, Irwin, PA) was hardened at 175 °C for 90 min. Dry ultrasonication and/or air blowing were used to remove the loosely adhering powder in the pores of the scaffolds. Scaffolds were then sintered[29] at 1250 °C in a conventional muffle furnace for 2 h (sintering cycles: 3 deg/min heating rate up to 120 °C; 1 h dwell time at 120 °C; then 3 deg/min heating rate up to 600 °C; 1 h dwell time at 600 °C; then 1 deg/min heating rate up to 1150 or 1250 °C; 2 h dwell time; 10 deg/min cooling rate). Figure 1a shows the schematic of 3D printing.[29]

2.2. Alendronate (AD) Loading and Polycaprolactone (PCL) Coating Preparation. PCL with an average molecular weight, M_w = 14000 (purchased from Sigma, St. Louis, MO, USA) and Alendronate (AD) (a generous gift from Pipeline Biotechnology, NJ, USA) were used in this study. The solution for PCL coating was prepared by dissolving 1 wt % PCL in acetone (w/v). Three different AD concentrations, 500, 800, and 1000 μg of AD per scaffold, were used to investigate the *in vitro* AD release behavior from PCL-coated scaffolds. AD-loaded scaffolds without any PCL coatings were used to compare the release kinetics with PCL-coated scaffolds. The solution for AD coating was prepared by dissolving AD in deionized water. AD coating was done by pipetting 50 μL of AD aqueous solution, such that this 50 μL either contained 500, 800, or 1000 μg of AD. For PCL-coated scaffolds, coating was done by pipetting 40 μL of 1 wt % PCL solution in acetone per scaffold.

For *in vivo* study, scaffolds were sterilized by autoclaving at 121 °C for 30 min prior to PCL or AD coating. AD was dissolved in sterilized nanopure water to prepare the AD-coating solution. AD coating was done by pipetting 20 μL of AD aqueous solution such that this 20 μL solution contained 2 μg of AD. Scaffolds were then dried overnight under a sterile hood. Scaffolds were then coated by pipetting 40 μL 1 wt % PCL solution in acetone. All coating procedure was carried out in a sterile environment.

2.3. Pore Size, Coating Morphology, and Mechanical Properties. Images for pore size measurement and surface morphologies of PCL-coated 3D printed TCP scaffolds were taken using a field-emission scanning electron microscope (FESEM) (FEI Inc., Hillsboro, OR, USA) followed by gold sputter-coating (Technics Hummer V, CA, USA). Pore size of the sintered scaffolds were calculated by averaging nine measurements for each pore size from three scaffolds (three different pores were selected from each scaffold for this measurement). Compressive strength and toughness analysis were performed to compare the mechanical properties between PCL-coated and without PCL-coated scaffolds. Compressive strength analysis was performed on the 3DP TCP scaffolds fabricated for *in vivo* implantation. A similar PCL coating procedure as described above for *in vivo* scaffolds was followed. Compressive strength of these 3DP TCP scaffolds with and without PCL coating was measured using a screw-driven universal testing machine (AG-IS, Shimadzu, Tokyo, Japan) with a constant crosshead speed of 0.33 mm/min, and the

calculation was performed based on the maximum load at failure and initial scaffold dimension. Ten samples (n = 10) were used from each composition for compressive strength analysis. Toughness was calculated from the area under the stress vs strain plot.

2.4. *In Vitro* Alendronate Release. Alendronate (AD) release behavior was investigated in two different 0.1 M pH buffers. A pH 7.4 phosphate buffer and pH 5.0 acetate buffer were used to mimic the physiological pH and slightly acidic micro environment right after surgery, respectively. A pH probe was used for pH measurement to keep the pH within ±0.05. Any loosely bound AD was washed off from each sample before starting the release study using 1 mL of DI water twice. Final AD content per scaffold was determined by subtracting AD amount in this 2 mL rinse aliquot from the loaded amount. Three samples from each concentration of AD (500 μg, 800 μg, and 1000 μg AD per scaffold) with and without PCL coating were placed in 2 mL of pH 7.4 phosphate buffer and pH 5 acetate buffer in separate vials, respectively, with appropriate labeling followed by keeping at 37 °C under 150 rpm constant shaking. Buffer solutions were changed at 2, 4, 6, 12, 24, 48, 72, 96, 120, and 168 h. Every time release media was replaced by a freshly prepared 2 mL fresh buffer solution. AD concentration was determined spectrophotometrically at 293 nm wavelength via complex formation with Fe (III) ions using a Biotek Synergy 2 SLFPTAD microplate reader (Biotek, Winooski, VT, USA).

2.5. Change in Phase, Dissolution, and Surface Morphology after Release. Any phase change in the scaffolds was monitored by X-ray diffraction (XRD) using a Philips PW 3040/00 Xpert MPD system (Philips, Eindhoven, The Netherlands) with Cu K$_\alpha$ radiation and Ni filter. Scanning range of 20° to 45° at a step size of 0.05° and a count time of 1 s per step were used. Surface morphologies of all scaffolds after release were observed under a field emission scanning electron microscope as described above followed by air drying of the scaffolds at ambient temperature for 72 h at the end of the release experiment. A Shimadzu AA-6800 atomic absorption spectrophotometer (AAS) (Shimadzu, Kyoto, Japan) was used for Ca^{2+} ion concentration analysis in the release media.

2.6. *In Vivo* Study. Twenty-four male Sprague-Dawley rats (Simonsen Laboratories, Gilroy, CA, USA) with an average body weight of 280 to 300 g for 6 and 10 weeks were used in the present study. The experimental detail for the animal study is presented in Figure S1 in the Supporting Information. The *in vivo* animal study plan is in agreement with ISO 10993-6:2009 (Biological evaluation of medical devices, Part 6: Tests for local effects after implantation).

2.6.1. Surgery and Implantation Procedure. Six different scaffold compositions, namely, (i) TCP (bare TCP), (ii) TCP + AD (AD-loaded TCP), (iii) TCP + PCL (PCL-coated TCP), (iv) TCP + PCL + AD, (v) TCP + AD + PCL, and (vi) TCP + AD + PCL + AD were tested in the distal femoral defect of Sprague-Dawley rats (Charles Rivers Laboratories International, Inc., Wilmington, MA, USA). The rats were kept in individual cages with free access to food and water in a temperature and humidity controlled room with alternating 12:12 light−dark (LD) cycle. After acclimatization, a distal femoral cortical defect (3 mm diameter) was created. A 3 mm drill bit was used to create the defect in the distal femur followed by washing the defect cavity by physiological saline to remove any remaining bone fragments. A mixture of IsoFlo (isoflurane, USP, Abbott Laboratories, North Chicago, IL, USA) and oxygen (Oxygen USP, A-L Compressed Gases Inc., Spokane, WA, USA) were used to anesthetize the rats. All animals underwent a bilateral surgery. VICRYL (polyglactin 910) synthetic absorbable surgical suture (Ethicon Inc., Somerville, NJ, USA) was used to close the wounds after the surgery. After the study time points (6 and 10 weeks), rats were euthanized by halothane overdosing in a bell jar, followed by administration of an intracardiac 70% potassium chloride injection. All surgical and animal care procedures were conducted in accordance with the protocol approved by the Institutional Animal Care and Use Committee (IACUC), Washington State University.

2.6.2. Histomorphology. All bone-implant samples for histological analysis were fixed in 10% buffered formalin solutions or 72 h. The specimens were then either dehydrated for undecalcified tissue
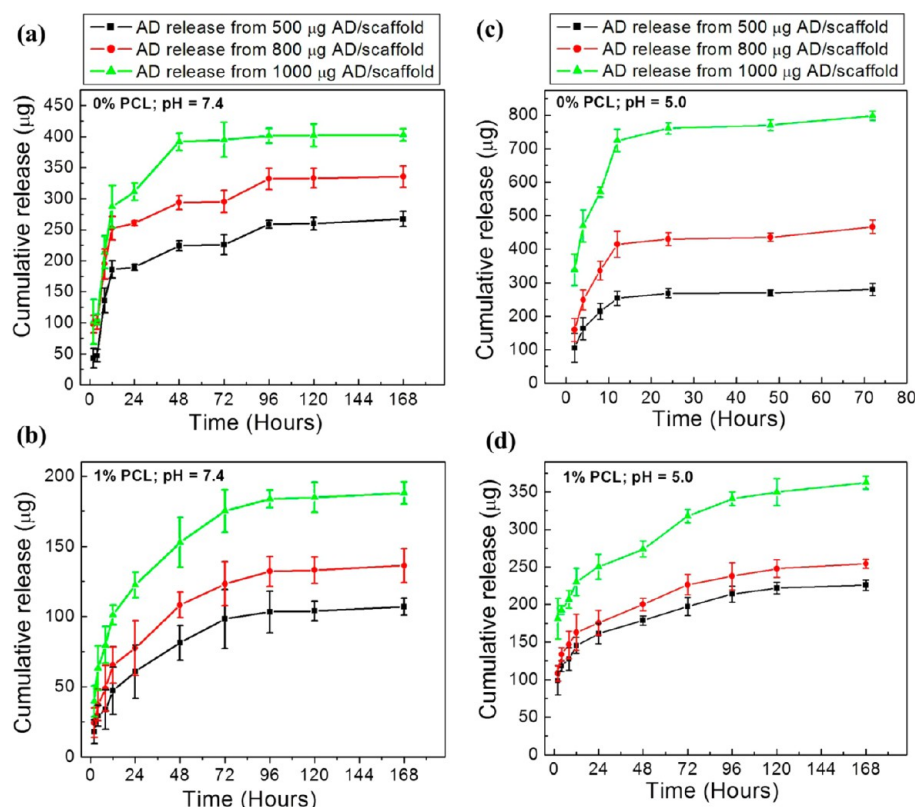
Figure 2. Cumulative AD release at pH 7.4 phosphate buffer (a, b) and at pH 5.0 acetate buffer (c, d) from bare TCP (i.e., no PCL coating: indicated by 0% PCL) scaffolds (a, c), and PCL-coated (1 % PCL in acetone (w/v) solution was used for coating) scaffolds (b, d).

sections preparation or decalcified and then dehydrated for decalcified tissue sections preparation.

2.6.2.1. Hematoxylin and Eosin (H&E) Staining. After formalin fixation, samples were kept in 14 % ethylenediaminetetraacetic acid (EDTA) until the samples were demineralized. At the end of decalcification, samples were dehydrated in graduated ethanol (30%, 50%, 70%, 90%, and 100%), ethanol−xylene (1:1), and 100% xylene. Samples were then paraffin embedded, and 5 to 10 μm thick tissue sections were cut using a microtome. Paraffin embedded decalcified tissue sections were deparaffined and used for hematoxylin and eosin (H&E) staining.

2.6.2.2. Tartrate Resistant Acid Phosphatase (TRAP) Staining. TRAP staining was performed following a previously reported procedure.[33] Formalin fixed paraffin embedded tissue sections were deparaffined followed by incubation at 37 °C for 30 min in preheated sodium acetate buffer of pH 4.9 with naphthol AS-BI phosphate (Sigma). The temperature was controlled by keeping the buffer solution in a water bath. Slides were then kept in pararosaniline and sodium nitrate solution for 5 min at room temperature, and then rinsed by distilled water. Finally, counterstaining was performed by keeping the slides into hematoxylin for 30 s, followed by dehydration and mounting with a coverslip.

2.6.2.3. Histomorphometric Analysis. ImageJ software (National Institute of Health) was used for newly formed bone area (bone area/ area of the entire tissue section, %) and TRAP activity (TRAP positive area/area of the entire tissue section, %) analysis from 800 μm width and 800 μm height tissue sections ($n = 8$). H&E stained tissue sections and TRAP stained sections were used for new bone area and TRAP activity analysis, respectively.

2.7. Statistical Analysis. Quantitative data for sintered pore size, compressive strength, new bone area and TRAP activity are expressed as mean ± standard deviation. Statistical analysis was performed on compressive strength, new bone area and TRAP activity using student's t-test, and P value <0.05 was considered significant.

3. RESULTS

3.1. Microstructure, PCL-Coating Morphology, and Mechanical Properties. Interconnected designed macropores are clearly visible in the sintered bare TCP and PCL-coated TCP scaffolds. Designed pore size of the scaffolds was 350 μm. Sintered pore sizes were 311 ± 5.9 μm.[28] Figure 1b presents the photograph of a sintered 3DP TCP scaffold. Figure 1c and d shows surface morphology of the uncoated and PCL-coated 3DP TCP scaffolds. The PCL solution concentration, 1 wt % PCL in acetone, and the solution volume for coating were selected to obtain a thin coating without blocking the designed macro pores and leaving some micro pores. PCL coating made the TCP surface more roughened through the flake like PCL coating (as shown in Figure S2 in the Supporting Information). Surface morphology of the PCL-coated scaffolds showed rough surface morphology along with the presence of many intrinsic micro pores. Compressive strength and toughness comparison between uncoated and PCL-coated 3DP TCP scaffolds are presented in Figure S3 in the Supporting Information showing 5.74 ± 1.34 and 5.58 ± 1.21 MPa compressive strength for these scaffolds, respectively. PCL coating did not cause an increase in compressive strength of the 3DP TCP scaffolds. However, PCL coating on these 3DP pure TCP scaffolds caused a noticeable increase in the toughness, from 4.23 × 10^{-6} to 8.51 × 10^{-6} J/m^3 as shown in Figure S3 in the Supporting Information.

3.2. *In Vitro* Alendronate and Ca^{2+} Release, Coating Morphology, and Phase. Figure 2a and b shows the cumulative AD release at pH 7.4 phosphate buffer from uncoated and PCL-coated 3DP TCP scaffolds, respectively. AD release from the PCL-coated scaffolds showed better perform-ance compared to uncoated TCP in terms of sustained and
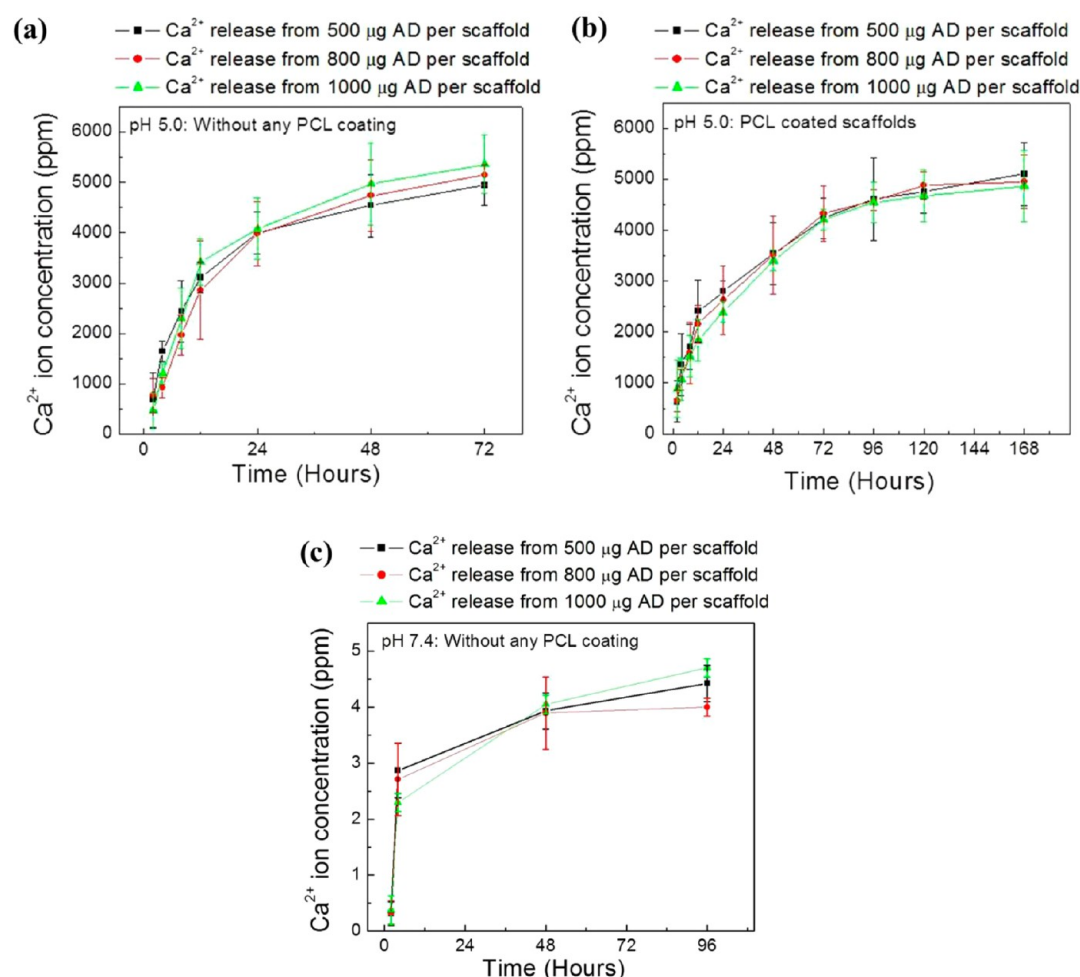
Figure 3. Cumulative Ca^{2+} ion release in the release media from bare TCP (a), PCL-coated TCP scaffolds (b) at pH 5.0, and from bare TCP scaffolds at pH 7.4 (c) as a function of release time (Ca^{2+} release was not observed at all-time points). No detectable Ca^{2+} ion release was observed from PCL-coated scaffolds at pH 7.4 within the ppm (μg/mL) range.

controlled release over the study period. Both initial and final AD release was decreased from the scaffolds with PCL coating. AD release at pH 5.0 acetate buffer from uncoated and PCL-coated TCP scaffolds are presented in Figure 2c and d, respectively. Increased level of drug concentration in the PCL coating resulted in increased total AD release at both pH 5 and pH 7.4.

However, total AD release was higher at pH 5.0 compared to pH 7.4 from both uncoated and PCL-coated scaffolds. This is an indication that release media pH has a significant role on the release kinetics from the PCL coating. The influence of TCP dissolution on AD release was evaluated by measuring Ca^{2+} ion concentration in the release media. Ca^{2+} ion release at pH 5.0 from the uncoated and PCL-coated 3DP TCP scaffolds are presented in Figure 3a and b, respectively. Ca^{2+} ion release at pH 5.0 from uncoated TCP is presented in Figure 3a for up to 72 h because all scaffolds disintegrated at this pH before 96 h. This type of scaffolds disintegration was not observed from PCL-coated scaffolds. A lower Ca^{2+} ion release rate was observed from PCL-coated scaffolds than uncoated TCP scaffolds at pH 5.0. Figure 3c shows the Ca^{2+} ion release from bare TCP scaffolds at pH 7.4 for 2, 4, 48, and 96 h. Other time points did not show any Ca^{2+} ion release within the detectable range [ppm (μg/mL) level]. Ca^{2+} ion release was

not observed at any time points from PCL-coated scaffolds at pH 7.4 within the detectable range.

Figure 4 shows the surface morphology of the uncoated and PCL-coated 3DP TCP scaffolds before and after AD release at both pH 7.4 and 5.0. Calcium deficient apatite formation was observed on uncoated TCP scaffolds at pH 7.4 after 7 d release (Figure 4c). PCL coating morphology did not show any change after 7 d AD release at pH 7.4. Individually separated grains were observed in bare TCP scaffolds at pH 5.0. Both PCL coating degradation and TCP scaffold dissolution was observed in PCL-coated 3DP TCP scaffolds at pH 5.0. Acidic release media caused the degradation of the PCL coating.

XRD patterns of the as-received β-TCP powder, TCP scaffolds sintered at 1250 °C for 2 h, and after AD release at pH 5.0 and 7.4 are presented in Figure 5. Our previously reported results showed that sintering at 1250 °C for 2 h of these 3D printed TCP scaffolds resulted in 25% α-TCP (JCPDS 09-0348) and 75% β-TCP (JCPDS 09-0169) because of high temperature phase transformation from β to α. The major peak for α-TCP disappeared after AD release at pH 5.0. This is due to high dissolution of α-TCP compared to β-TCP. All α-TCP was dissolved and caused the disintegration of the scaffolds. The intensity of the Major peak for α-TCP was decreased at pH 7.4 due to low dissolution of α-TCP at pH 7.4. Other than this, no phase change was observed.
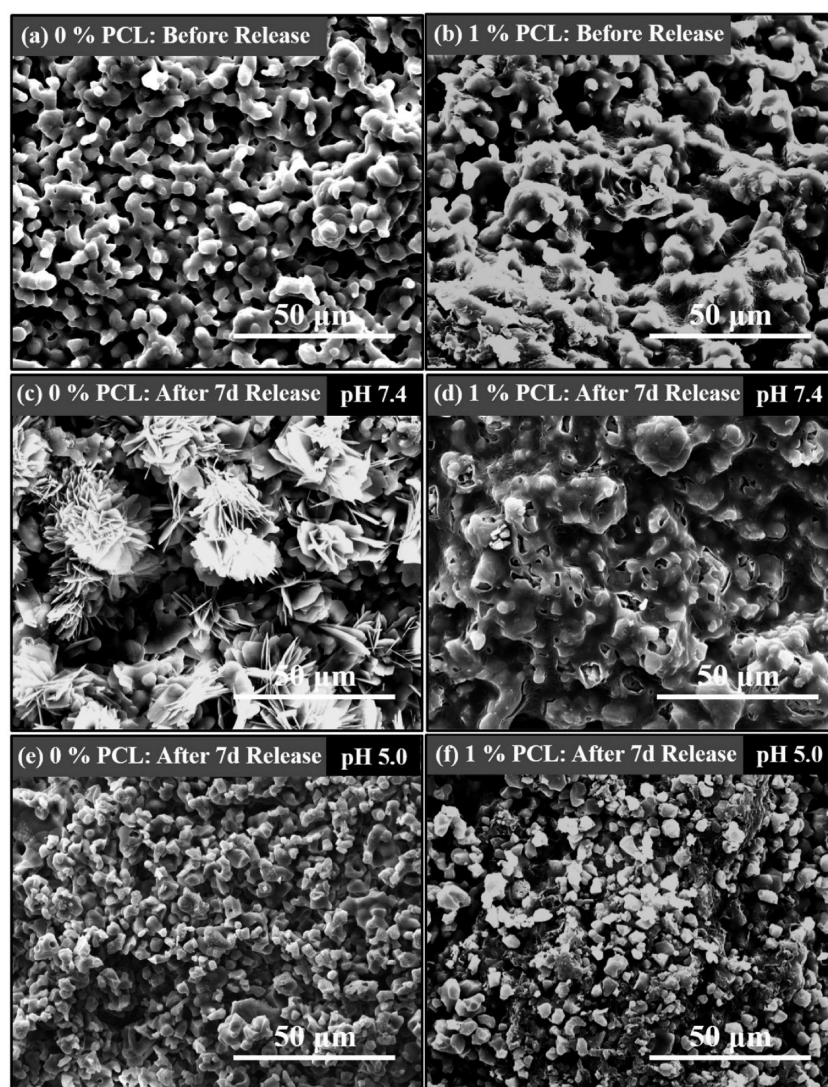
Figure 4. Surface morphology of bare TCP (i.e., no PCL coating: indicated by 0% PCL) and PCL-coated (1 % PCL in acetone (w/v) solution was used for coating) TCP scaffolds before and after AD release at pH 7.4 and 5.0: (a) bare TCP before AD release, (b) PCL coated TCP before AD release, (c) bare TCP after AD release at pH 7.4, (d) PCL-coated TCP scaffold after AD release at pH 7.4, (e) bare TCP after AD release at pH 5.0, and (f) PCL-coated TCP scaffold after AD release at pH 5.0.

3.3. Histomorphology and Histomorphometry.

Histological evaluation was performed at 6 and 10 weeks to evaluate the influence of AD and PCL coating on new bone formation. Figure 6 shows hematoxylin and eosin (H&E) staining of decalcified tissue sections, which shows new bone formation inside the macro and micro pores of the scaffolds. Acellular regions shown in the figure are derived from the demineralization process of the scaffolds. Newly formed bone observed by H&E staining showed a clear distinction between 6 weeks and 10 weeks. Newly formed bone after 10 weeks was more compact in nature compared to after 6 weeks. Histomorphometric analysis of newly formed bone area comparison after 6 and 10 weeks are presented in Figure 7. No significant difference in bone formation was noticed between uncoated and PCL-coated TCP after 6 and 10 weeks. All scaffolds with AD showed a significant increase in bone formation at both time points compared to bare TCP and TCP with PCL coating. TCP + AD + PCL scaffolds showed maximum bone formation after 6 weeks, which was significantly higher than TCP + AD scaffolds. However, new bone formation after 10 weeks induced

by TCP + AD and TCP + AD + PCL was similar. TCP + AD + PCL scaffolds showed a significantly increased bone formation compared to TCP + PCL + AD scaffolds.

Activity of TRAP positive cells after 6 and 10 weeks are shown in Figure S4 in the Supporting Information. TRAP positive cells were observed inside the all TCP scaffolds after 6 weeks suggesting bone resorbing osteoclasts activity. AD containing scaffolds showed lower TRAP activity compared to bare TCP and TCP+PCL scaffolds. TCP with only AD showed the least TRAP activity after 6 weeks. Activity of TRAP positive cells was increased in bare TCP, TCP+PCL and TCP+AD scaffolds after 10 weeks, where all other remaining samples showed decreasing TRAP positive cells activity after 10 weeks. Histomorphometric analysis of TRAP positive cells activity comparison after 6 and 10 weeks are presented in Figure 8. Bare TCP and TCP + PCL showed almost similar TRAP positive cells activity after 6 weeks, but bare TCP showed maximum TRAP positive cells activity after 10 weeks with a significant difference compared to TCP + PCL. TCP + AD scaffolds showed the least TRAP positive cells activity after
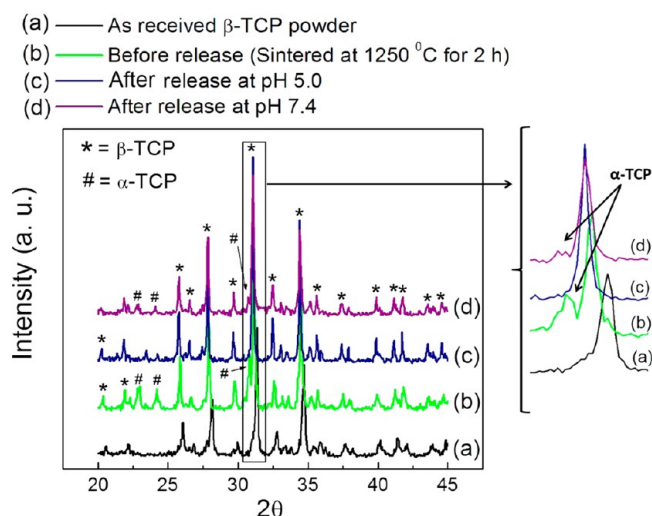
(a) —— As received β-TCP powder
(b) —— Before release (Sintered at 1250 °C for 2 h)
(c) —— After release at pH 5.0
(d) —— After release at pH 7.4

Figure 5. XRD patterns of the 3DP TCP scaffolds before and after AD release. The major peak for α-TCP disappeared after AD release at pH 5.0 due to high dissolution of α-TCP as shown in (c). The intensity of the Major peak for α-TCP was decreases at pH 7.4 because of low dissolution of α-TCP at pH 7.4 as shown in (d). Other than this, no phase change was observed.

6 weeks, which is significantly lower than the TRAP positive cells activity in TCP + AD + PCL scaffolds. However, a similar TRAP positive cells activity was observed after 10 weeks between TCP + AD and TCP + AD + PCL scaffolds.

4. DISCUSSION

Making tissue engineering constructs hierarchically porous is an effort to mimic native tissue structure and functionality. The presence of 3D interconnected porosity provides adequate cell penetration and vascularization for the ingrowth tissue.[29,34] Tissue engineering scaffolds with multiscale porosity (both macro- and micropore) facilitates enhanced bone regeneration,[35,36] and strong mechanical interlocking can be achieved between the scaffold and host tissue from large surface area.[29] Although the minimum recommended macropore diameter for effective osteogenesis is 100 μm, macropore diameters between 200 and 350 μm are recommended for effective vascularization and bone tissue ingrowth.[37] The sintered macropore diameter used in this study was 311 ± 5.9 μm, which is in the range of optimum size for effective tissue regeneration.[29] Among most CaPs, tricalcium phosphates (TCPs) are widely used because of their resorbable properties.[18] A higher solubility of TCP compared to other CaPs allows them to degrade faster. Between the two polymorphs of TCP, α-TCP degrades faster than β-TCP, and both α- and β-TCP are widely used in bone tissue engineering.[29,38] Previously, we showed that both α- and β-TCP were present in these 3DP β-TCP scaffolds sintered at 1250 °C.[29]

Initial burst release is very common for drugs or biomolecules delivered from CaP based delivery system.[6,39,40] Initial burst and uncontrolled release of the drug from the implant surface are not beneficial, and will not serve the purpose of local delivery for effective treatment. Drug adsorption and release from CaPs primarily depends on chemical and electrostatic interactions between CaPs and drug molecules.[1,41,42] In most cases, weak electrostatic interactions keep the drug entities bound to the adsorbed surface.[6] A big difference of BPs with other drugs is that BPs

can strongly bind to CaPs surface. The strong bonding between BPs and CaPs results from a chemical exchange of the phosphate group.[43] After the first layer of drug molecules adsorb through phosphate group exchange, subsequent layers remain bound to the surface by weak electrostatic interactions.[41] An initial burst release is thus still observed for BP delivery from CaPs. Biodegradable polymer coating can be very effectual drug delivery approach for sustained and controlled delivery by preventing burst release kinetics.[1,6,25,44]

We have recently reported that both polymer concentration in the coating solution and the pH of the release media can influence the drug release kinetics.[6] Higher AD release at lower pH (5.4) and lower AD release at higher pH (7.4) indicated a favorable interaction between AD and release media at lower pH or AD and PCL. Phobicity of the polymer-drug and polymer solubility in the release media also influence the release kinetics.[6,45] The higher Ca^{2+} ion release rate from bare TCP scaffolds and their disintegration at pH 5.0 after 72 h is due to much higher solubility of TCP at acidic pH than at neutral and basic pH.[46] PCL coating delayed TCP dissolution by hindering TCP from direct contact with a harsh acidic environment. This is further supported from the surface morphology and the phase analysis of the scaffolds after release. Calcium deficient apatite formation on bare TCP at pH 7.4 indicates Ca ion release caused by the TCP dissolution was re-precipitated. This was the reason for detecting Ca ion at the initial and the middle of the release time points. Higher dissolution of bare TCP at pH 5.0 created individual grain separation, and ultimately caused disintegration of the scaffolds. The disappearance of the α-TCP major peak at pH 5.0 could be due to much higher dissolution of α-TCP than the β-TCP. The decreased intensity of the α-TCP major peak at pH 7.4 and the apatite formation indicates the dissolution of α-TCP and re-precipitation as calcium deficient apatite.

Drug release depends on diffusion, chemical processes, matrix degradation, and external or electronic processes.[1,6,41,47] Usually diffusion process dominates drug release kinetics because matrix degradation is a slower process than the diffusion.[6] In this study, we see matrix degradation dominated AD release at pH 5.0 and diffusion dominated AD release at pH 7.4. The phobicity of the drug and polymer along with the solubility of the polymer can also play a dominant role. Both alendronate (sodium salt) and alendronic acid are hydrophilic, soluble in water, and cause an unfavorable interaction between AD (both salt and acid form) and PCL. Thus, the dissociation of AD from TCP caused either by TCP dissolution or driven by equilibrium shift is the rate limiting factor. Because the next step is the diffusion of AD from the PCL matrix in the coating caused by the unfavorable interaction between AD and PCL. In the absence of PCL coating, AD release from uncoated 3DP TCP scaffold is governed by the rate limiting step. These rate limiting and non-rate limiting steps are schematically shown in Figure 9.

Increased peri-implant bone density formation was noticed by Peter et al.,[48] when zoledronate (a member of BPs family) was applied on hydroxyapatite-coated titanium implants. Another study by Garbuz et al.[49] reported increased gap filling, bone ingrowth, and total bone formation, when alendronate was applied on calcium phosphate coated tantalum implants. Both studies[48,49] reported that around 2 μg of BPs were most effective for *in vivo* bone ingrowth resulting enhanced implant-host tissue integration. Thus, 2 μg of AD per scaffold was applied in this study, except TCP + AD + PCL + AD, where 4
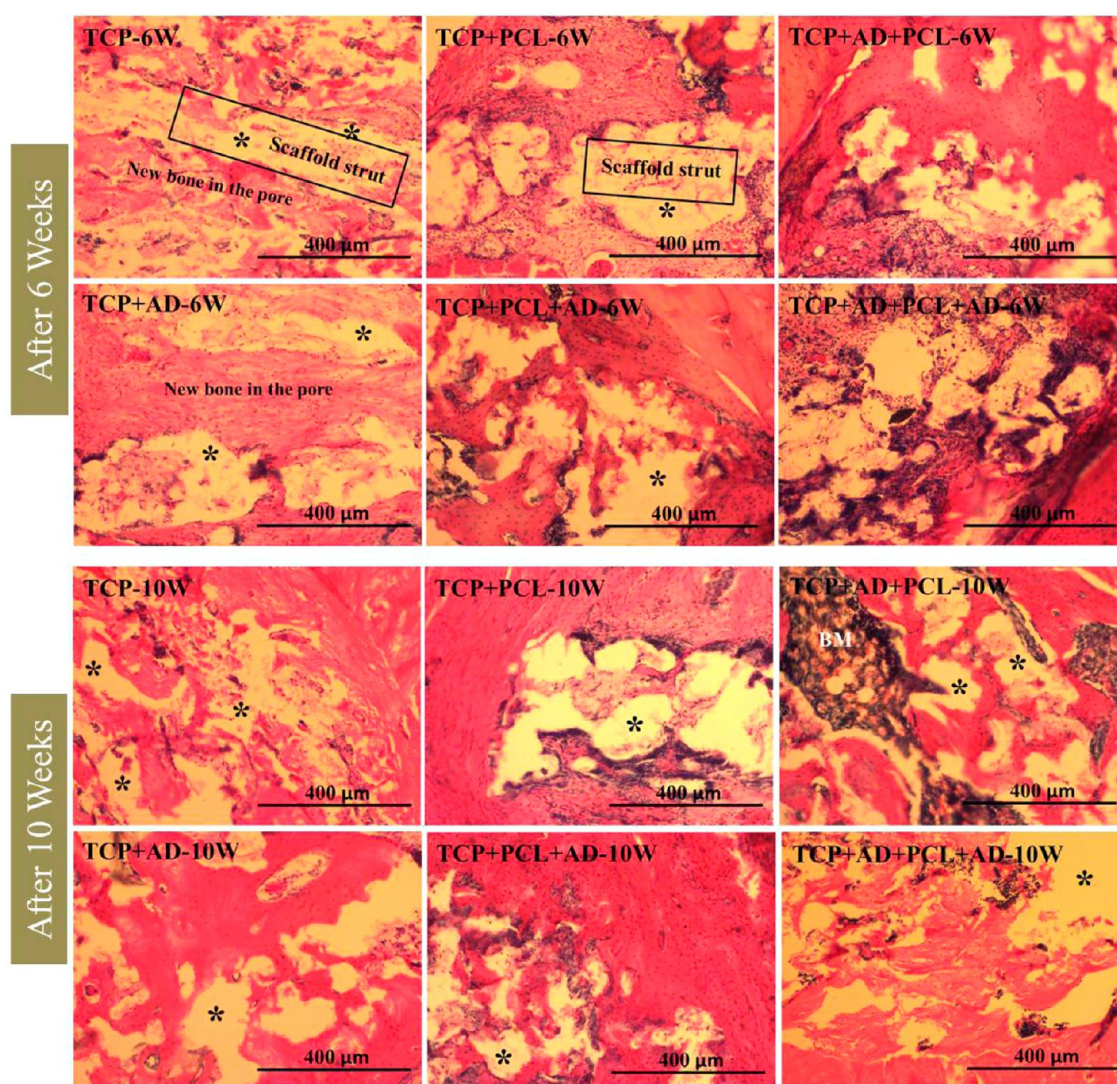
9961

dx.doi.org/10.1021/am501048n | ACS Appl. Mater. Interfaces 2014, 6, 9955−9965

Figure 6. Photomicrographs of representative histological sections after hematoxylin and eosin (H&E) staining of decalcified tissue sections showing the development of bone formation after 6 and 10 weeks. BM = Bone marrow. Asterisk (*) indicates acellular regions derive from scaffold.

μg of AD was applied in two layers. H&E staining of decalcified tissue sections showed (Figure 6) excellent ingrowth of newly formed bone inside the micro and macro pores of the 3D printed scaffolds. This clearly shows the advantage of tissue engineering scaffolds with multiscale porosity. Interconnected network-like structure of the newly formed bone could form due to the designed interconnected porosity in the 3D printed TCP scaffolds. *In vitro* hFOB cells also showed good cell adhesion and proliferation in the scaffolds of all compositions (Figure S5 in the Supporting Information). Histomorphometric analysis showed that TCP+PCL scaffolds promoted slightly higher bone formation compared to bare TCP after 6-weeks (Figure 7). Although there was no difference in new bone area between bare TCP and TCP + PCL scaffolds after 10 weeks, which is consistent with the *in vitro* cell culture results (Figure S6 in the Supporting Information). PCL coating made the TCP surface more roughened, and the flake like PCL coating simulated a 3D micro environment. It has been reported that the 3D structure of PCL such as roughened surface and nanofibers facilitates proliferation and osteogenic differentiation of human mesenchymal stem cells (hMSCs).[50,51] Therefore, the roughened surface due to PCL coating might have

facilitated osteogenic differentiation and proliferation of osteoprogenitor cells present in the bone marrow. Unlike hFOB cell density results (Figure S6 in the Supporting Information), new bone area was higher in TCP + PCL + AD scaffolds compared to bare TCP and TCP + PCL scaffolds. This is probably because of the *in vivo* action of AD on bone resorbing osteoclast cells. A significant increase in bone formation was observed in TCP + AD + PCL scaffolds compared to TCP + AD scaffolds after 6 weeks. This is probably due to the prevention of initial burst release as a result of PCL coating. As a result, AD was possibly released for a longer time period. No difference in newly formed bone area between TCP + AD and TCP + AD + PCL scaffolds after 10 weeks also suggests that it is the initial controlled release that played the key role for early bone formation, which is crucial for rapid wound healing and implant−host tissue integration.

TRAP (tartrate resistant acid phosphatase) is the main acid secreted by mature osteoclasts during bone resorption.[52] Bare TCP and TCP + PCL scaffolds showed the highest TRAP positive cells activity as shown by the histomorphometric analysis after 6 weeks (Figure 8). A significantly higher TRAP positive cells activity after 10 weeks in bare TCP compared to
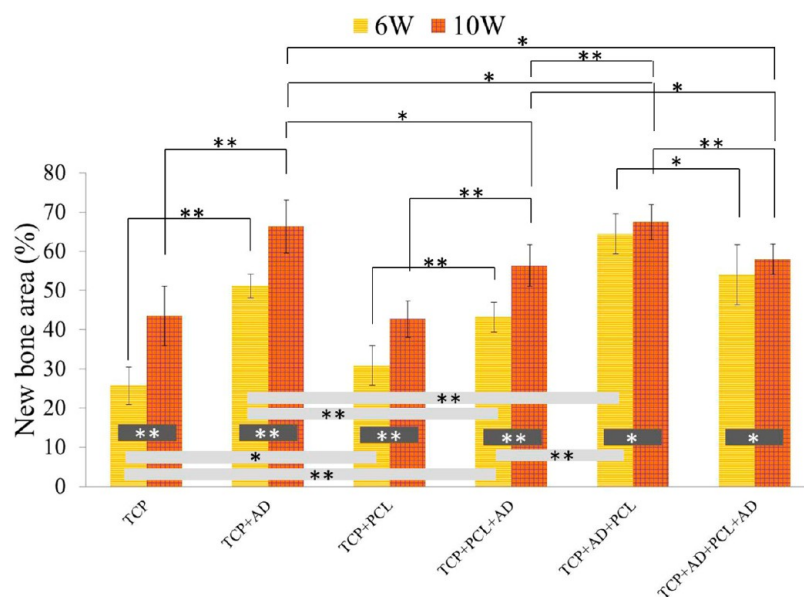
9962

dx.doi.org/10.1021/am501048n | *ACS Appl. Mater. Interfaces* 2014, 6, 9955−9965

Figure 7. Histomorphometric analysis showing total new percent bone formation comparison between the treatment and control groups (**$p <$ 0.05, *$p >$ 0.05, $n = 8$ tissue sections of 800 μm width and 800 μm height each).
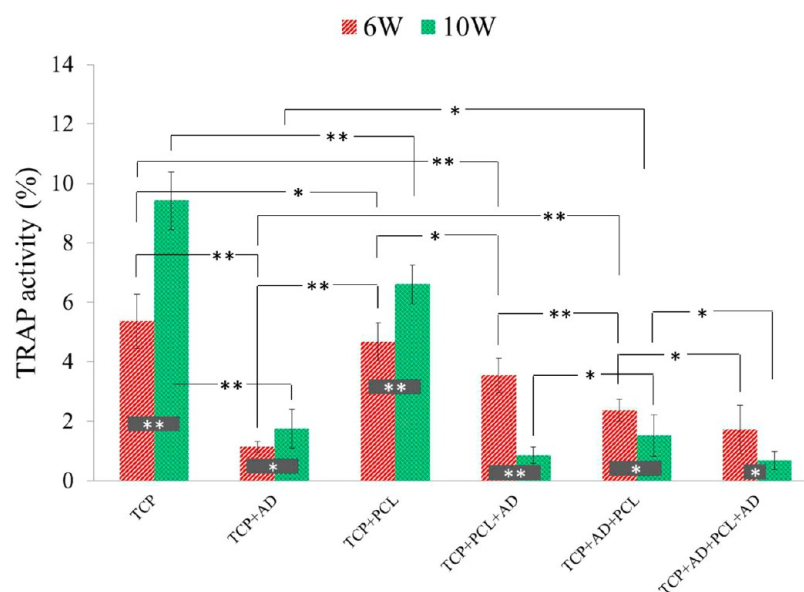

Figure 8. Histomorphometric analysis showing percent TRAP activity comparison between the treatment and control groups (**$p < 0.05$, *$p > 0.05$, $n = 8$ tissue sections of 800 μm width and 800 μm height each).

TCP + PCL is probably because of higher dissolution of bare TCP, which initiated greater osteoclasts activities. A lower TRAP positive cells activity in all scaffolds with AD indicates the inhibition of osteoclasts activity by AD. A higher TRAP positive cells activity in TCP + PCL + AD amongst all scaffolds with AD is probably due to an initial rapid release of all drugs. After this initial release, these TCP + PCL + AD scaffolds acted more like that of TCP + PCL scaffolds without any AD. A higher TRAP positive cells activity in TCP + AD + PCL compared to TCP + AD after 6 weeks could be due to sustained AD release for longer time caused by the PCL coating. This might have inhibited osteoclasts activity and promoted higher bone formation. *In vitro* AD release shows that PCL coating can effectively be used for controlled and sustained drug delivery without any unfavorable effects on cells.

In vivo results show that local AD delivery from PCL-coated 3DP TCP scaffolds could further induce increased early bone formation. Therefore, biodegradable polymer coated 3DP TCP scaffolds have great potential use in bone tissue engineering for controlled and sustained drug delivery applications for early wound healing through increased osteogenesis.

■ CONCLUSIONS

This study examines the effect of PCL coating on *in vitro* alendronate (AD) release kinetics, and local AD delivery on *in vivo* bone formation from polycaprolactone (PCL) coated 3D printed tricalcium phosphate scaffolds. A controlled AD release was observed from 3DP PCL-coated scaffolds, whereas uncontrolled release associated with burst release was observed from uncoated 3DP TCP scaffolds. PCL coating also showed
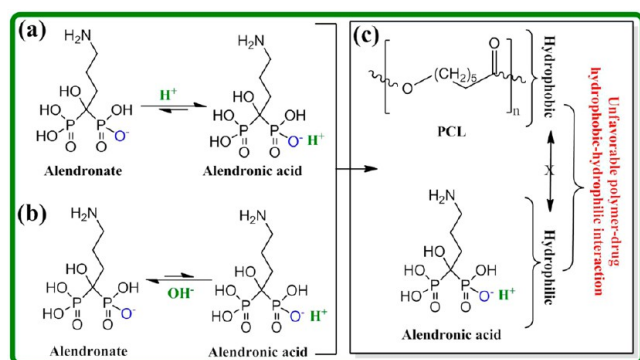
Figure 9. Schematic representation of the rate limiting steps for AD (salt or acid form) release. AD is liberated from the TCP surface in the presence of acidic (a) or basic (b) release medium, which is caused by the rate limiting TCP dissolution and/or equilibrium driven shift. In presence of PCL coating, final AD release is caused by the diffusion of AD from PCL coating through the unfavorable interaction between AD and PCL (non-rate limiting step) (c). In absence of PCL coating, AD release is governed by the rate limiting steps.

its beneficial effect in protecting structural integrity of the TCP scaffolds from high dissolution in acidic environments. AD release was dominated by the rate limiting dissociation of AD from TCP caused by either TCP dissolution or driven by equilibrium shift. Finally, AD release from the PCL matrix in the coating was caused by the unfavorable interaction between AD and PCL. In the absence of PCL coating, AD release was entirely governed by the rate limiting step. All scaffolds with AD showed higher bone formation and reduced TRAP positive cells activity compared to bare TCP and TCP coated with only PCL. TCP + PCL scaffolds did not show any adverse effects on *in vitro* osteoblast cells proliferation and *in vivo* bone formation because of the presence of PCL. TCP + AD scaffolds showed enhanced bone formation compared to bare TCP scaffolds after 6 weeks. Both histomorphology and histomorphometric analysis revealed maximum bone formation after 6 weeks when TCP + AD scaffolds were coated with PCL. No noticeable difference in new bone formation was observed after 10 weeks between TCP + AD and TCP + AD + PCL scaffolds. This early wound healing through bone tissue regeneration is probably caused by a gradual AD release as a result of inhibition of initial burst release by PCL coating. Bare TCP showed the highest TRAP positive cells activity at both time points. These results suggest that PCL-coated 3DP TCP scaffolds can effectively be used for local drug delivery from for enhanced osteogenesis for early wound healing.

ASSOCIATED CONTENT

Ⓢ Supporting Information

In vivo animal study experimental plan, PCL coating morphology, compressive strength and toughness comparison between PCL-coated and non-PCL-coated 3DP pure TCP scaffolds, photomicrographs of TRAP staining, *in vitro* cell culture procedure and results (including SEM micrographs of hFOB cells, and cell proliferation data from MTT assay) are provided in the supporting information. This material is available free of charge via the Internet at http://pubs.acs.org/.

AUTHOR INFORMATION

Corresponding Author

*E-mail: sbose@wsu.edu. Phone: (509) 335-7461.

REFERENCES

(1) Bose, S.; Tarafder, S. Calcium Phosphate Ceramic Systems in Growth Factor and Drug Delivery for Bone Tissue Engineering: A Review. *Acta Biomater.* **2012**, *8*, 1401–1421.

(2) Ezra, A.; Golomb, G. Administration Routes and Delivery Systems of Bisphosphonates for the Treatment of Bone Resorption. *Adv. Drug Delivery Rev.* **2000**, *42*, 175–195.

(3) Frommelt, L. Principles of Systemic Antimicrobial Therapy in Foreign Material Associated Infection in Bone Tissue, With Special Focus on Periprosthetic Infection. *Injury* **2006**, *37*, S87–S94.

(4) Acharya, G.; Park, K. Mechanisms of Controlled Drug Release From Drug-Eluting Stents. *Adv. Drug Delivery Rev.* **2006**, *58*, 387–401.

(5) Radin, S.; Campbell, J. T.; Ducheyne, P.; Cuckler, J. M. Calcium Phosphate Ceramic Coatings as Carriers of Vancomycin. *Biomaterials* **1997**, *18*, 777–782.

(6) Tarafder, S.; Nansen, K.; Bose, S. Lovastatin Release from Polycaprolactone Coated β-Tricalcium Phosphate: Effects of pH, Concentration and Drug–Polymer Interactions. *Mater. Sci. Eng. C* **2013**, *33*, 3121–3128.

(7) Lin, J. H. Bisphosphonates: A Review of Their Pharmakokinetic Properties. *Bone* **1996**, *18*, 75–85.

(8) Nancollas, G. H.; Tang, R.; Phipps, R. J.; Henneman, Z.; Gulde, S.; Wu, W.; Mangood, A.; Russell, R. G. G.; Ebetino, F. H. Novel Insights into Actions of Bisphosphonates on Bone: Differences in Interactions with Hydroxyapatite. *Bone* **2006**, *38*, 617–627.

(9) Liberman, U. A.; Weiss, S. R.; Bröll, J.; Minne, H. W.; Quan, H.; Bell, N. H.; Rodriguez-Portales, J.; Downs, R. W.; Dequeker, J.; Favus, M.; Seeman, E.; Recker, R. R.; Capizzi, T.; Santora, A. C.; Lombardi, A.; Shah, R. V.; Hirsch, L. J.; Karpf, D. B. Effect of Oral Alendronate on Bone Mineral Density and The Incidence of Fractures in Postmenopausal Osteoporosis. *N. Engl. J. Med.* **1995**, *333*, 1437–1444.

(10) Rodan, G. A.; Reszka, A. A. Bisphosphonate Mechanism of Action. *Curr. Mol. Med.* **2002**, *2*, 571–577.

(11) Coxon, F. P.; Thompson, K.; Rogers, M. J. Recent Advances in Understanding the Mechanism of Action of Bisphosphonates. *Curr. Opin. Pharmacol.* **2006**, *6*, 307–312.

(12) Reszka, A. A.; Rodan, G. A. Mechanism of Action of Bisphosphonates. *Curr. Osteoporos. Rep.* **2003**, *1*, 45–52.

(13) Van Beek, E.; Löwik, C.; Van Der Pluijm, G.; Papapoulos, S. The Role of Geranylgeranylation in Bone Resorption and Its Suppression by Bisphosphonates in Fetal Bone Explants In Vitro: A Clue to the Mechanism of Action of Nitrogen-Containing Bisphosphonates. *J. Bone Miner. Res.* **1999**, *14*, 722–729.

(14) Rogers, M. J.; Gordon, S.; Benford, H. L.; Coxon, F. P.; Luckman, S. P.; Monkkonen, J.; Frith, J. C. Cellular and Molecular Mechanisms of Action of Bisphosphonates. *Cancer* **2000**, *88*, 2961–2978.

(15) Roelofs, A. J.; Thompson, K.; Gordon, S.; Rogers, M. J. Molecular Mechanisms of Action of Bisphosphonates: Current Status. *Clin. Cancer Res.* 2006, 12, 6222s–6230s.

(16) Kim, C. W.; Yun, Y. P.; Lee, H. J.; Hwang, Y. S.; Kwon, I. K.; Lee, S. C. In Situ Fabrication of Alendronate-Loaded Calcium Phosphate Microspheres: Controlled Release for Inhibition of Osteoclastogenesis. *J. Controlled Release* 2010, 147, 45–53.

(17) Giger, E. V.; Castagner, B.; Leroux, J.-C. Biomedical Applications of Bisphosphonates. *J. Controlled Release* 2013, 167, 175–188.

(18) Bandyopadhyay, A.; Bernard, S.; Xue, W.; Bose, S. Calcium Phosphate-Based Resorbable Ceramics: Influence of MgO, ZnO, and SiO$_2$ Dopants. *J. Am. Ceram. Soc.* 2006, 89, 2675–2688.

(19) Banerjee, S. S.; Tarafder, S.; Davies, N. M.; Bandyopadhyay, A.; Bose, S. Understanding The Influence of MgO and SrO Binary Doping on The Mechanical and Biological Properties of β-TCP Ceramics. *Acta Biomater.* 2010, 6, 4167–4174.

(20) Bose, S.; Tarafder, S.; Banerjee, S. S.; Davies, N. M.; Bandyopadhyay, A. Understanding In Vivo Response and Mechanical Property Variation in MgO, SrO and SiO$_2$ Doped β-TCP. *Bone* 2011, 48, 1282–1290.

(21) Seeley, Z.; Bandyopadhyay, A.; Bose, S. Tricalcium Phosphate Based Resorbable Ceramics: Influence of NaF and CaO Addition. *Mater. Sci. Eng. C* 2008, 28, 11–17.

(22) Habraken, W. J. E. M.; Wolke, J. G. C.; Jansen, J. A. Ceramic Composites as Matrices and Scaffolds For Drug Delivery in Tissue Engineering. *Adv. Drug Delivery Rev.* 2007, 59, 234–248.

(23) Manzano, M.; Vallet-Regí, M. Revisiting Bioceramics: Bone Regenerative and Local Drug Delivery Systems. *Prog. Solid State Chem.* 2012, 40, 17–30.

(24) Xue, W.; Bandyopadhyay, A.; Bose, S. Polycaprolactone Coated Porous Tricalcium Phosphate Scaffolds for Controlled Release of Protein for Tissue Engineering. *J. Biomed. Mater. Res., Part B* 2009, 91, 831–838.

(25) Kim, H. W.; Knowles, J. C.; Kim, H. E. Hydroxyapatite/ Poly(Caprolactone) Composite Coatings on Hydroxyapatite Porous Bone Scaffold for Drug Delivery. *Biomaterials* 2004, 25, 1279–1287.

(26) Moioli, E. K.; Clark, P. A.; Xin, X.; Lal, S.; Mao, J. J. Matrices and Scaffolds for Drug Delivery in Dental, Oral and Craniofacial Tissue Engineering. *Adv. Drug Delivery Rev.* 2007, 59, 308–324.

(27) Coombes, A. G. A.; Rizzi, S. C.; Williamson, M.; Barralet, J. E.; Downes, S.; Wallace, W. A. Precipitation Casting of Polycaprolactone for Applications in Tissue Engineering and Drug Delivery. *Biomaterials* 2004, 25, 315–325.

(28) Mattanavee, W.; Suwantong, O.; Puthong, S.; Bunaprasert, T.; Hoven, V. P.; Supaphol, P. Immobilization of Biomolecules on the Surface of Electrospun Polycaprolactone Fibrous Scaffolds for Tissue Engineering. *ACS Appl. Mater. Interfaces* 2009, 1, 1076–1085.

(29) Tarafder, S.; Balla, V. K.; Davies, N. M.; Bandyopadhyay, A.; Bose, S. Microwave-Sintered 3D Printed Tricalcium Phosphate Scaffolds for Bone Tissue Engineering. *J. Tissue Eng. Regen. Med.* 2013, 7, 631–641.

(30) Fielding, G. A.; Bandyopadhyay, A.; Bose, S. Effects of Silica and Zinc Oxide Doping on Mechanical and Biological Properties of 3D Printed Tricalcium Phosphate Tissue Engineering Scaffolds. *Dent. Mater.* 2012, 28, 113–122.

(31) Butscher, A.; Bohner, M.; Hofmann, S.; Gauckler, L.; Müller, R. Structural and Material Approaches to Bone Tissue Engineering in Powder-Based Three-Dimensional Printing. *Acta Biomater.* 2011, 7, 907–920.

(32) Sachlos, E.; Czernuszka, J. Making Tissue Engineering Scaffolds Work. *Eur. Cells Mater.* 2003, 5, 29–40.

(33) Jiang, X.; Kalajzic, Z.; Maye, P.; Braut, A.; Bellizzi, J.; Mina, M.; Rowe, D. W. Histological Analysis of GFP Expression in Murine Bone. *J. Histochem. Cytochem.* 2005, 53, 593–602.

(34) Bölgen, N.; Yang, Y.; Korkusuz, P.; Güzel, E.; El Haj, A. J.; Pişkin, E. Three-Dimensional Ingrowth of Bone Cells Within Biodegradable Cryogel Scaffolds in Bioreactors at Different Regimes. *Tissue Eng., Part A* 2008, 14, 1743–1750.

(35) Lan Levengood, S. K.; Polak, S. J.; Wheeler, M. B.; Maki, A. J.; Clark, S. G.; Jamison, R. D.; Wagoner Johnson, A. J. Multiscale Osteointegration As A New Paradigm For The Design Of Calcium Phosphate Scaffolds For Bone Regeneration. *Biomaterials* 2010, 31, 3552–3563.

(36) Hing, K. A.; Annaz, B.; Saeed, S.; Revell, P. A.; Buckland, T. Microporosity Enhances Bioactivity of Synthetic Bone Graft Substitutes. *J. Mater. Sci.: Mater. Med.* 2005, 16, 467–475.

(37) Bose, S.; Roy, M.; Bandyopadhyay, A. Recent Advances in Bone Tissue Engineering Scaffolds. *Trends Biotechnol.* 2012, 30, 546–554.

(38) Carrodeguas, R. G.; De Aza, S. α-Tricalcium Phosphate: Synthesis, Properties and Biomedical Applications. *Acta Biomater.* 2011, 10, 3536–3546.

(39) Yoshinari, M.; Matsuzaka, K.; Hashimoto, S.; Ishihara, K.; Inoue, T.; Oda, Y.; Ide, T.; Tanaka, T. Controlled Release of Simvastatin Acid Using Cyclodextrin Inclusion System. *Dent. Mater. J.* 2007, 26, 451–456.

(40) Banerjee, S. S.; Bandyopadhyay, A.; Bose, S. Biphasic Resorbable Calcium Phosphate Ceramic for Bone Implants and Local Alendronate Delivery. *Adv. Eng. Mater.* 2010, 12, B148–B155.

(41) Tarafder, S.; Banerjee, S.; Bandyopadhyay, A.; Bose, S. Electrically Polarized Biphasic Calcium Phosphates: Adsorption and Release of Bovine Serum Albumin. *Langmuir* 2010, 26, 16625–16629.

(42) Dasgupta, S.; Bandyopadhyay, A.; Bose, S. Reverse Micelle-Mediated Synthesis of Calcium Phosphate Nanocarriers for Controlled Release of Bovine Serum Albumin. *Acta Biomater.* 2009, 5, 3112–3121.

(43) Roussière, H.; Fayon, F.; Alonso, B.; Rouillon, T.; Schnitzler, V.; Verron, E.; Guicheux, J.; Petit, M.; Massiot, D.; Janvier, P.; Bouler, J.-M.; Bujoli, B. Reaction of Zoledronate With β-Tricalcium Phosphate for the Design of Potential Drug Device Combined Systems. *Chem. Mater.* 2008, 20, 182–191.

(44) Kim, H.-W.; Knowles, J. C.; Kim, H.-E. Hydroxyapatite Porous Scaffold Engineered with Biological Polymer Hybrid Coating for Antibiotic Vancomycin Release. *J. Mater. Sci: Mater. Med.* 2005, 16, 189–195.

(45) Saylor, D. M.; Kim, C.; Patwardhan, D. V.; Warren, J. A. Modeling Microstructure Development and Release Kinetics in Controlled Drug Release Coatings. *J. Pharm. Sci.* 2009, 98, 169–186.

(46) Fernandez, E.; Gil, F. J.; Ginebra, M. P.; Driessens, F. C. M.; Planell, J. A.; Best, S. M. Production and Characterization of New Calcium Phosphate Bone Cements in the CaHPO$_4$–α-Ca$_3$(PO$_4$)$_2$ System: pH, Workability and Setting Times. *J. Mater. Sci.: Mater. Med.* 1999, 10, 223–230.

(47) Ginebra, M.-P.; Traykova, T.; Planell, J. A. Calcium Phosphate Cements: Competitive Drug Carriers for the Musculoskeletal System? *Biomaterials* 2006, 27, 2171–2177.

(48) Peter, B.; Pioletti, D. P.; Laïb, S.; Bujoli, B.; Pilet, P.; Janvier, P.; Guicheux, J.; Zambelli, P.-Y.; Bouler, J.-M.; Gauthier, O. Calcium Phosphate Drug Delivery System: Influence of Local Zoledronate Release on Bone Implant Osteointegration. *Bone* 2005, 36, 52–60.

(49) Garbuz, D. S.; Hu, Y.; Kim, W. Y.; Duan, K.; Masri, B. A.; Oxland, T. R.; Burt, H.; Wang, R.; Duncan, C. P. Enhanced Gap Filling and Osteoconduction Associated with Alendronate-Calcium Phosphate-Coated Porous Tantalum. *J. Bone Joint Surg. Am.* 2008, 90, 1090–1100.

(50) Kumar, G.; Waters, M. S.; Farooque, T. M.; Young, M. F.; Simon, C. G., Jr. Freeform Fabricated Scaffolds with Roughened Struts That Enhance Both Stem Cell Proliferation and Differentiation by Controlling Cell Shape. *Biomaterials* 2012, 33, 4022–4030.

(51) Kumar, G.; Tison, C. K.; Chatterjee, K.; Pine, P. S.; McDaniel, J. H.; Salit, M. L.; Young, M. F.; Simon, C. G., Jr. The Determination of Stem Cell Fate by 3D Scaffold Structures Through the Control of Cell Shape. *Biomaterials* 2011, 32, 9188–9196.

(52) Webster, T. J.; Ergun, C.; Doremus, R. H.; Siegel, R. W.; Bizios, R. Enhanced Osteoclast-Like Cell Functions on Nanophase Ceramics. *Biomaterials* 2001, 22, 1327–1333.